Chemical durability of bituminous geomembranes (BGMs) in heap leach pad applications

F. B. Abdelaal[1] and A. Samea[2]

[1]*Assistant Professor in Geotechnical and Geoenvironmental Engineering, Department of Civil Engineering, GeoEngineering Centre at Queen's-RMC, Queens University, Ellis Hall, Kingston, ON K7L 3N6, Canada, E-mail: fady.abdelaal@queensu.ca (corresponding author)*
[2]*Graduate student, Department of Civil Engineering, GeoEngineering Centre at Queen's-RMC, Queen's University, Ellis Hall, Kingston, ON K7L 3N6, Canada, E-mail: alireza.samea@queensu.ca*

Received 14 August 2022, accepted 03 April 2023, first published online 11 April 2023

ABSTRACT: The degradation behaviour of a 4.8 mm thick elastomeric bituminous geomembrane (BGM) immersed in pH 0.5, 9.5, and 11.5 synthetic mining solutions is examined over 26 months at 22, 40, 55 and 70°C. The low pH solution simulates the leach solutions found in copper, nickel, and uranium heap leach pads while the two high pH solutions simulate the chemistry and pH found in gold and silver heap leaching facilities. The mechanical, rheological, and chemical properties are examined at different incubation times to assess the degradation in the BGM at different temperatures. It is shown that the degradation rates of all properties are faster in pH 11.5 and 9.5 than in pH 0.5. Additionally, the BGM started to exhibit degradation in its mechanical properties even with a slightly degraded bitumen coat in all the mining solutions at elevated temperatures. The time to nominal failure of the BGM is predicted at different field temperatures using Arrhenius modelling. Due to the relatively fast degradation in the mechanical properties of the BGM, especially at temperatures above 50°C, the tensile strains in the BGM in the field should be limited so it can meet the required liner design life of heap leaching applications.

KEYWORDS: Geosynthetics, Bituminous geomembrane, Durability, Heap leach pads, Mining

REFERENCE: Abdelaal, F. B. and Samea, A. (2024). Chemical durability of bituminous geomembranes (BGMs) in heap leach pad applications. *Geosynthetics International*, **31**, No. 5, 506–523. [https://doi.org/10.1680/jgein.22.00333]

1. INTRODUCTION

Heap leaching is a common geoenvironmental application for geomembranes (GMBs) that is widely used for the recovery of gold, silver, copper, uranium, and nickel (Thiel and Smith 2004; John 2011). In this method, the ore is leached using acidic solutions with a pH range of 0.5–2 for the extraction of copper, uranium and nickel or alkaline solutions with a pH range of 9.5–12 for the extraction of gold and silver (Breitenbach and Thiel 2005; Lupo 2010; Abdelaal *et al*. 2011; Petersen 2016). The leach solution that contains the precious metal (called the pregnant leach solution (PLS)) is collected using a series of geopipes embedded in a coarse-grained layer overlying the pad and processed for metal recovery in a lined PLS pond (Thiel and Smith 2004; Lupo 2010; Abdelaal *et al*. 2011).

Geosynthetic barrier systems are typically used in the pad under the ore to protect the surrounding environment from the corrosive leaching solutions and to preserve the precious minerals being extracted. Due to the combination of high overburden pressures (in the case of static heap leaching), extreme pH of the PLS in contact with the liner, and elevated temperatures (sometimes >75°C), heap leaching is considered one of the most aggressive service environments for the GMB liner (Breitenbach and Thiel 2005; Scheirs 2009; Abdelaal *et al*. 2011; Rowe and Abdelaal 2016). Previous research examined the durability of polymeric geomembrane liners (e.g. Gulec *et al*. 2004; Abdelaal *et al*. 2011; Rowe and Abdelaal 2016; Abdelaal and Rowe 2017, 2023; Morsy and Rowe 2017) under the aggressive conditions of the heap leach applications. Recently, bituminous geomembranes (BGMs) have been introduced to mining applications due to their lower coefficient of thermal expansion, higher puncture resistance, and higher density relative to polymeric GMBs but there is a paucity of research into their long-term performance under the service conditions of heap leach pads (Scheirs 2009; Lazaro and Breul 2014; Daly and Breul 2017).

BGMs are manufactured by impregnating and coating a nonwoven polyester geotextile (NW-GTX) and a glass fleece layer with bitumen to give a relatively impervious

and flexible sheet (Peggs 2008). The upper surface of the BGM is typically coated with fine sand to increase the interface friction of the liner system, while a polyester film is bonded to the bottom side to prevent the adhesion of the turns of the BGM roll during storage and protect the BGM from upward root penetration during service (Lazaro and Breul 2014). Early BGMs were manufactured using oxidized bitumen to improve the temperature sensitivity of the bitumen coat (i.e. to raise the flow temperature and lower its low-temperature brittleness), but nowadays, the bitumen coat is stabilized with elastomers such as styrene-butadiene-styrene (SBS) (Touze-Foltz and Farcas 2017).

The performance of the BGMs as a barrier material relies on both the bitumen coat providing the waterproofing characteristics of the BGM and the reinforcement layers providing its mechanical properties (Touze-Foltz and Farcas 2017; Samea and Abdelaal 2023). The effect of moisture and different aqueous solutions on the chemical properties of bitumen was previously studied in pavement research by monitoring the changes in the rheological behaviour and chemical structure of the bitumen (e.g. Ma *et al.* 2011; Hung *et al.* 2017; Pang *et al.* 2018; Wei *et al.* 2019; Zhang *et al.* 2020; Zou *et al.* 2021; Ding *et al.* 2022; Feng *et al.* 2022). It was shown that exposing the bitumen to aqueous solutions can result in its oxidation due to the reaction of the bitumen with the oxygen molecules dissolved in the aqueous solutions. Alternately, water-soluble components of bitumen can dissolve into the aqueous solutions during exposure (Yang *et al.* 2020; Zou *et al.* 2021). Both mechanisms were found to be accelerated by exposing the bitumen to alkaline solutions (Pang *et al.* 2018; Zou *et al.* 2021). Although these studies simulated the bitumen exposure to corrosive solutions, they used ageing methods designed for asphalt pavements (rolling thin film oven and/or pressure ageing vessel) involving relatively short incubation times that cannot simulate the longer design life of BGM in heap leaching applications. Additionally, these studies did not involve the degradation of the other BGM components.

The only attempt found in the literature for investigating the chemical durability of BGMs in heap leaching applications was a study by Esford and Janssens (2014), who examined the chemical durability of an elastomeric BGM for the primary liner of a weak sulfuric acid PLS pond. The BGM coupons were immersed in a diluted acidic solution with 20% sulfuric acid and 100 ppm kerosene for three years at room temperature. Monitoring the physical and mechanical properties of the BGM showed that the BGM did not exhibit any significant degradation as a result of exposure to the solution. Based only on one temperature and one solution, this study concluded that the BGM was suitable for use as the primary liner in this application.

Samea and Abdelaal (2023) also investigated the durability of BGMs in air and deionized (DI) water at different elevated temperatures for two years using immersion tests. While the results provided insights into the degradation behaviour of BGMs at elevated temperatures, they cannot be used to estimate the longevity of the BGM liners in heap leaching applications with extreme pHs. Thus, the first objective of this paper is to investigate the long-term performance of an elastomeric BGM at different temperatures when exposed to extremely low and high pH solutions simulating the PLS typically found in heap leach pad applications. The second objective is to use time-temperature superposition modelling to predict the time to nominal failure of the BGM at the typical field temperatures of heap leach pads.

2. EXPERIMENTAL INVESTIGATION

2.1. Immersion solutions

Three different synthetic mining solutions (Table 1) were used in the current study to simulate the extreme pH and metal concentration of the PLS in different heap leaching applications. The solutions were prepared by mixing different inorganic salts with DI water ($pH \approx 6.5$). Either sodium hydroxide (15 M) or 98% sulfuric acid was titrated to achieve the desired pH of the solution. PLS1 with pH 0.5 simulates the chemistry and pH of solutions found in copper, uranium, and nickel heap leaching (Rowe and Abdelaal 2016). PLS2, and PLS3 with pH of 9.5 and 11.5, respectively, simulate the pH of the leaching solutions found in gold and silver heap leaching and some low-level radioactive waste leachates (Abdelaal and Rowe 2017; Tian *et al.* 2017). The solutions were replaced every two months to ensure a constant pH during the entire duration of the study.

Table 1. Chemical composition of the different mining solutions (mg/l except for pH)

Analyte[a]	PLS 1[b]	PLS 2[c]	PLS 3[c]
Nominal pH	0.5	9.5	11.5
Aluminium	5000	<1.0	<1.0
Arsenic	<0.03	0.9	0.9
Barium	<0.05	0.1	0.1
Cadmium	1.7	<0.025	<0.025
Calcium	515	0.42	0.64
Copper	87	9	9
Cobalt	20	0.03	0.03
Iron	710	<0.05	<0.05
Magnesium	3300	4	2.8
Molybdenum	<0.05	0.68	0.56
Nickel	7.6	<0.3	<0.3
Lead	1.4	<0.03	<0.03
Lithium	1000	<0.05	<0.05
Potassium	<0.2	173	181
Silver	<1.0	0.3	0.3
Sodium	50	60	138
Zinc	62	0.02	0.02
Chloride	5100	<0.5	<0.5
Hydroxides	0	43	9440
Oxides	0	0.59	0.59
Sulphate	68 000	300	300

[a]Metal ions were analyzed using an inductively coupled plasma-mass spectrometer (ICP-MS), while the anions were analyzed using Ion chromatography (IC).
[b]Values after Rowe and Abdelaal (2016).
[c]Values after Abdelaal and Rowe (2017).

Table 2. Initial properties of the examined BGM

Property[a]	Method	Unit	Mean ± SD[b]
Designator	—	—	TERANAP 531 TP 4M
Nominal thickness	ASTM D5199	mm	4.8 ± 0.120 (4.6)
Glass mat reinforcement	—	g/m^2	50[c]
Mass per unit area of the nonwoven geotextile reinforcement	ASTM D5261	g/m^2	275[c]
Mass per unit area of the BGM	ASTM D5261	g/m^2	5410[c]
Machine direction maximum tensile strength σ_M	ASTM D7275	kN/m	33.1 ± 0.422 (25.5)
Machine direction elongation at σ_M	ASTM D7275	mm	51 ± 1.8 (33)
Cross machine maximum tensile strength σ_M	ASTM D7275	kN/m	29.5 ± 0.887 (23)
Cross machine elongation at σ_M	ASTM D7275	mm	52 ± 1.5 (35.7)
Puncture resistance F_M	ASTM D4833	N	690 ± 41.91 (555)
Puncture elongation at F_M	ASTM D4833	mm	14.35 ± 0.933
Glass transition temperature of bitumen tack coat	ASTM E2602	°C	−24.2 ± 1.48

[a]10 replicates were examined for each property.
[b]Values in parentheses show the minimum specified value by the manufacturer for this BGM.
[c]Values from the manufacturer datasheet.

2.2. Materials examined

The BGM examined comprises a reinforcement layer that includes a polyester NW-GTX with a mass per unit area of 275 g/m^2 and a glass fleece sheet with a mass per unit area of 50 g/m^2 impregnated and coated with SBS-modified bitumen. The BGM is 4.8 mm thick and is recommended by the manufacturer for high-stress geoenvironmental applications (e.g. mining applications). The top surface of the BGM is treated with sand, while the bottom surface has a polyester anti-root film. Table 2 shows the different ASTM index tests performed to obtain the initial properties of the BGM and the recommended minimum values for these properties by the manufacturer for this BGM. In addition, the NW-GTX (Table 3) used in the manufacturing of the BGM was examined to compare its long-term performance to the BGM.

Table 3. Initial properties of the examined NW-GTX

Property[a]	Method	Unit	Mean ± SD
Nominal thickness	ASTM D5199	mm	1.1 ± 0.128
Surface mass per unit area	ASTM D5261	g/m^2	263 ± 4.36
Machine direction maximum tensile strength	ASTM D5035	kN/m	13.4 ± 1.33
Machine direction elongation	ASTM D5035	mm	48 ± 3.7
Cross machine maximum tensile strength	ASTM D5035	kN/m	10.5 ± 0.866
Cross machine elongation	ASTM D5035	mm	55 ± 1.2
Puncture resistance	ASTM D4833	N	627 ± 62.37
Puncture elongation	ASTM D4833	mm	16.79 ± 0.665
Glass transition temperature (°C)	ASTM E2602	°C	82.86 ± 2.27

[a]10 replicates were examined for each property.

2.3. Accelerating ageing and index testing

The jar immersion technique, in which coupons of the geomembrane are immersed in a jar filled with a synthetic solution, is widely used to accelerate the ageing of GMBs in the laboratory by exposing all sides of the GMB to aggressive media at elevated temperatures (e.g. Hsuan and Koerner 1998; Sangam and Rowe 2002; Müller and Jacob 2003; Abdelaal *et al*. 2011; Ewais *et al*. 2014; Rowe and Abdelaal 2016; Tian *et al*. 2017; Morsy *et al*. 2020; Abdelaal and Rowe 2023). This technique allows the estimation of the degradation times in the different properties of the GMB until the nominal failure of the material is reached. Time to nominal failure for geosynthetics is typically assessed as the time taken for a GMB property to decrease to 50% of the initial or the specified value (Hsuan and Koerner 1998; Rowe 2020). This is different from the GMB service life that is related to the loss of its hydraulic barrier function (i.e. time to rupture) that cannot be directly estimated from immersion tests since they do not simulate the demand on the GMB (i.e. stresses and strains) or the composite liner exposure in the field. However, immersion tests can be used to examine the chemical durability of the GMB and the effect of the exposure conditions, such as elevated temperature or the chemistry of the exposure media.

While the immersion tests accelerate the degradation of polymeric GMBs due to the exposure of all sides to the solution, for BGMs, exposure from the edges can directly expose the core NW-GTX to the immersion solutions. Samea and Abdelaal (2019) investigated the effect of exposing the NW-GTX to the immersion solutions by examining the degradation of BGM coupons that were sealed with BGM strips welded to their four edges and BGM coupons with exposed edges (unsealed). The results showed a substantially slower degradation in the mechanical properties of the sealed BGM coupons in different incubation solutions at elevated temperatures relative to the unsealed coupons with exposed NW-GTX at the coupon edges. Thus, before initiating the long-term immersion experiments, the BGM coupons (250 × 150 mm) were sealed using the same method reported by Samea and Abdelaal (2019) so that the coupons are only exposed to the solution from the top (bitumen coat) and the bottom (polymeric film) surfaces of the BGM. The sealed BGM coupons were placed in stainless steel containers filled with the PLS (with a surface area of the BGM per solution

volume = 450 cm^2/l) and incubated at 22, 40, 55 and 70°C. In addition, the NW-GTX used in the manufacturing of the BGM examined was incubated in the three solutions at 70°C. Due to the insignificant contribution of the polymeric film to the mechanical properties of BGM, it was not aged and tested separately (Samea and Abdelaal 2023). The BGM and the NW-GTX coupons were periodically extracted and used to monitor the changes in mechanical, rheological, and chemical properties of the samples using the different index tests discussed below.

2.3.1. *Modulated differential scanning calorimetry*

The changes in the glass transition temperature (T_g) of the bitumen were monitored to infer the change in the bitumen structure due to ageing (e.g. Masson and Polomark 2001; Kriz *et al.* 2007; Sá Da Costa *et al.* 2010; Wang *et al.* 2019a; Kaya *et al.* 2020). In this study, T_g of the bitumen top coat of the unaged and aged BGMs was measured, using a TA Instruments Modulated Differential Scanning Calorimeter (MDSC250), equipped with a refrigerated cooling system (RCS120), according to the inflection method (ASTM E2602). For each data point, three 5–8 mg specimens were extracted from the whole thickness of the bitumen top coat. Each specimen was placed in a Tzero hermetic pan sealed with hermetic lids and examined in the MDSC under a constant flow (50 ml/min) of nitrogen. To eliminate the thermal history of the samples, the sealed pans were pre-heated from room temperature to 170°C and annealed for 15 min. This was followed by quenching the samples to −110°C at a rate of 10°C/min then reheating to 170°C at a rate of 5°C/min while modulating the temperature with an amplitude of ±0.75°C and a period of 60 s.

2.3.2. *Dynamic shear rheometer*

The dynamic shear rheometer (DSR) is typically used to monitor the effect of ageing on the rheological properties of bitumen due to the changes in its chemical structure (e.g. Airey 2003; Lu *et al.* 2008; Wu *et al.* 2009; Ali *et al.* 2013; Ding *et al.* 2022). To characterize the viscous and elastic behaviour of BGM, complex shear modulus (G^*) and phase angle (δ) were measured in the linear viscoelastic region (LVE) of all unaged and aged BGM samples using an Anton Paar MCR 102 rheometer. G^* is defined as the ratio of the absolute shear stress and the resulting shear strain, while δ is the offset between the applied shear stress and resulting shear strain from a dynamic oscillation measurement (Airey 2003). For each data point, the rheological properties of three specimens were measured under the normal force constant control mode (1 N) at 55°C using a 25 mm parallel plate at a fixed frequency of 10 rad/s and under a strain level of 0.01% to 60%.

2.3.3. *Fourier transform infrared spectroscopy*

Fourier transform infrared spectroscopy (FTIR) is used to assess the increase in the carbonyl functional group due to oxidative degradation of the bitumen and the decrease in the butadiene functional group due to consumption of the SBS copolymer of polymer-modified bitumen (e.g. Lu and Isacsson 1999; Lamontagne *et al.* 2001; Zhang *et al.* 2011; Aguiar-Moya *et al.* 2017; Tauste *et al.* 2018; Kaya *et al.* 2020). A Thermo Scientific Nicolet iS20 spectrum is used to assess the spectra in the range of 4000 cm^{-1} to 400 cm^{-1} with a scan frequency of 32 and 4 cm^{-1} resolution. To remove the sand particles and NW-GTX fibres in the bitumen, samples of the whole bitumen thickness were extracted and dissolved in toluene (10% by weight), and then the bitumen solution was placed on potassium bromide (KBr) disks before the test to dry. To examine the effect of ageing on the functional groups of the bitumen and SBS copolymer, changes in the carbonyl C = O (centred around 1700 cm^{-1}) and the butadiene double bonds C = C (centred around 968 cm^{-1}) characteristic bands were monitored for three different specimens at each sampling event. The C = O band was used to monitor the oxidation of the entire bitumen coat, whereas the C = C band was used to monitor the degradation of the chain segments in the butadiene phase of the SBS. The carbonyl and butadiene indices that reflect the average changes in these functional groups with ageing relative to the unaged bitumen (e.g. Lamontagne *et al.* 2001; De Sá Araujo *et al.* 2013; Gao *et al.* 2013; Feng *et al.* 2022) were calculated viz:

$$I_{C=O} = \frac{\text{Area of the carbonyl band centered around } 1700\,\text{cm}^{-1}}{\Sigma\text{Area of the spectral bands between 4000 and } 600\,\text{cm}^{-1}} \quad (1)$$

$$I_{SBS} = \frac{\text{Area of the carbonyl band centered around } 968\,\text{cm}^{-1}}{\Sigma\text{Area of the spectral bands between 4000 and } 600\,\text{cm}^{-1}} \quad (2)$$

where $I_{C=O}$ = carbonyl index, I_{SBS} = butadiene index.

2.3.4. *Mechanical index tests*

To examine the effect of ageing on the mechanical properties of BGM, the tensile test (ASTM D7275) and puncture test (ASTM D4833/D4833M) were conducted in parallel in both the machine and cross-machine directions on unaged and aged BGM specimens at different temperatures and incubation durations. Ten specimens were examined to assess the unaged tensile and puncture properties of the BGM. For the aged samples, only two tensile specimens and one puncture specimen were examined at different incubation times to ensure the availability of samples during the entire duration of the long-term study to assess the changes in the BGM properties with time. The changes in the maximum (peak) tensile stress and the corresponding elongation of the BGM were monitored using a Zwick Roell universal testing machine (Model Z020) with a 50 mm/min separation rate. For the NW-GTX, the tensile properties were measured according to the ASTM D5035 test method at a strain rate of 300 mm/min. For the puncture test, the maximum puncture force and corresponding elongation of the BGM samples were measured using a GDS loading machine at a strain rate of 50 mm/min. The maximum (peak) stresses and corresponding elongations were used in this study to assess the mechanical properties of the BGM and the NW-GTX instead of the break stress and elongation as specified in the ASTM D7275, ASTM

D4833/D4833M, and ASTM D5035 test methods. This is because the peak values represent the onset of the NW-GTX failure that governs the mechanical properties of the BGM. Additionally, this allows the comparison of the degradation in the mechanical properties of the BGM to the NW-GTX samples that were separately incubated under the same conditions.

3. RESULTS AND DISCUSSION

3.1. Effect of pH on the chemical and rheological properties of BGM at 70°C

3.1.1. *Glass transition temperature*

In all three solutions, T_g decreased upon incubation with the increase in the incubation time, implying a change in the bitumen structure due to oxidative degradation in the mining solutions (Figure 1). The fastest change in T_g was in PLS2 and PLS3 with the high pH in which T_g decreased upon incubation from −24.2°C to reach the lowest T_g values of the bitumen of −37°C (Samea and Abdelaal 2023) after 24 and 19 months, respectively. In PLS1, the change in T_g was slower than in DI water (pH ≈ 6.5) in which the values were retained at the initial values for the first 7 months, then linearly decreased to around −29°C after 26 months of incubation. While the T_g decreased in all three solutions, the results suggest that increasing the pH from 0.5 to 11.5 resulted in more oxidative degradation in the bitumen coat. However, given the scatter in the data, the effect of increasing the pH from 6.5 to 11.5 was insignificant on the T_g at 70°C.

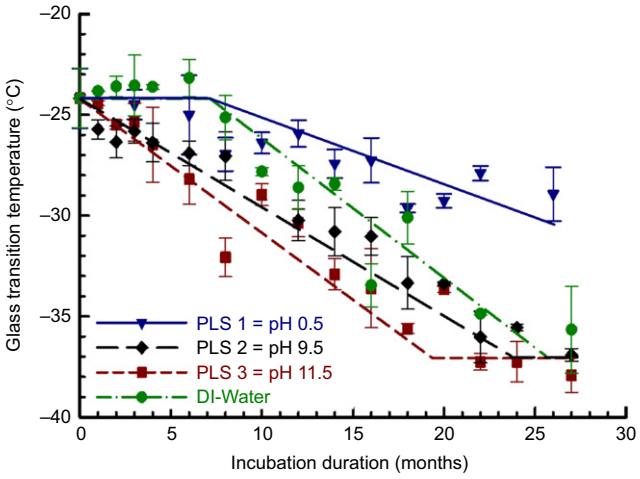

Figure 1. Variation in T_g with incubation time at 70°C in PLS1, PLS2, and PLS3. Data in DI-Water are from Samea and Abdelaal (2023). Unless otherwise noted, the data points presented in all the figures represent the mean value, while the error bars represent the ±1 standard deviation of the data

3.1.2. *Complex shear modulus and phase angle*

Ageing in the mining solutions at 70°C resulted in different changes in both G^* and δ of the aged BGM samples (Figure 2). In PLS1, the G^* slightly increased with ageing while d did not change during the 26 months of exposure, implying that the BGM maintained the viscous and elastic components of its unaged structure. In the PLS2 and PLS3, G^* gradually increased upon incubation to reach 2- and 2.5-fold the initial G^*, respectively after 26 months. At the same time, δ decreased by 30% in PLS2 and 40% in PLS3. The changes in G^* and δ in the alkaline solutions were slightly higher than the changes reported by Samea and Abdelaal (2023) for immersion in DI water. This highlights the effect of alkaline and neutral solutions on the bitumen that resulted in a higher shift in its rheology towards a less viscous and more elastic behaviour than the acidic solution.

3.1.3. *Carbonyl and butadiene indexes*

Incubation in both acidic and alkaline media increased the $I_{C=O}$ of the unaged bitumen (0.0024) with the ageing time, while the I_{SBS} was reduced due to the degradation of the butadiene segments (Figure 3). After 26 months of exposure to PLS1, the $I_{C=O}$ increased by a factor of 4.3, while in PLS2 and PLS3, it increased to reach 7.5 and 9 times the initial values, respectively. Similarly, I_{SBS} showed more degradation of the SBS copolymer in PLS2 and

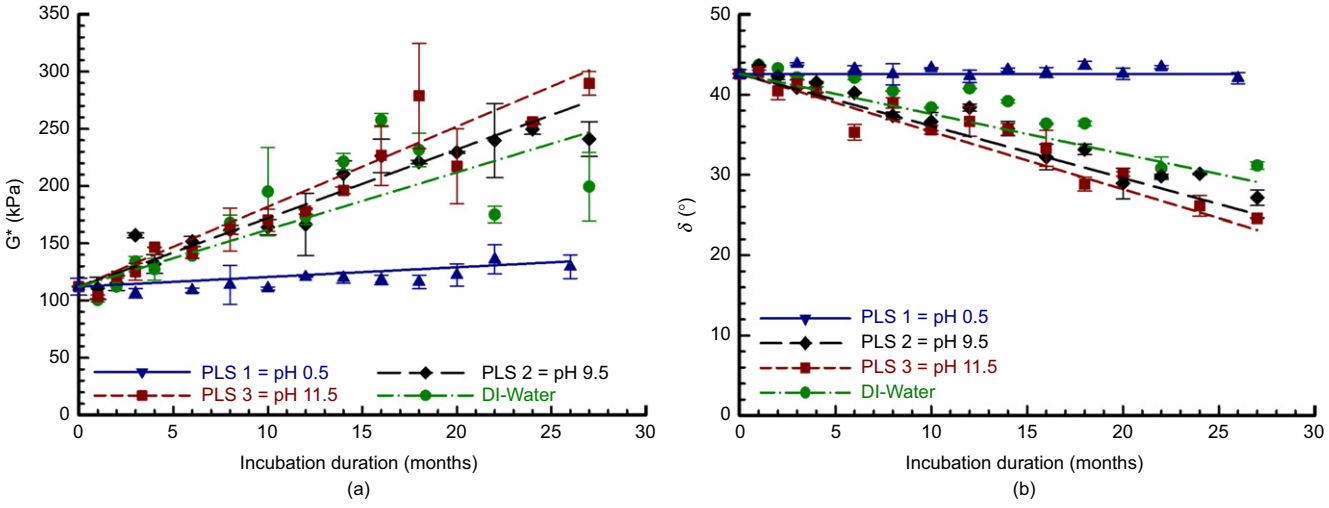

Figure 2. Variation of the G^* and δ with incubation time at 70°C in PLS1, PLS2, and PLS3: (a) G^*; (b) δ. Data in DI-Water are from Samea and Abdelaal (2023)

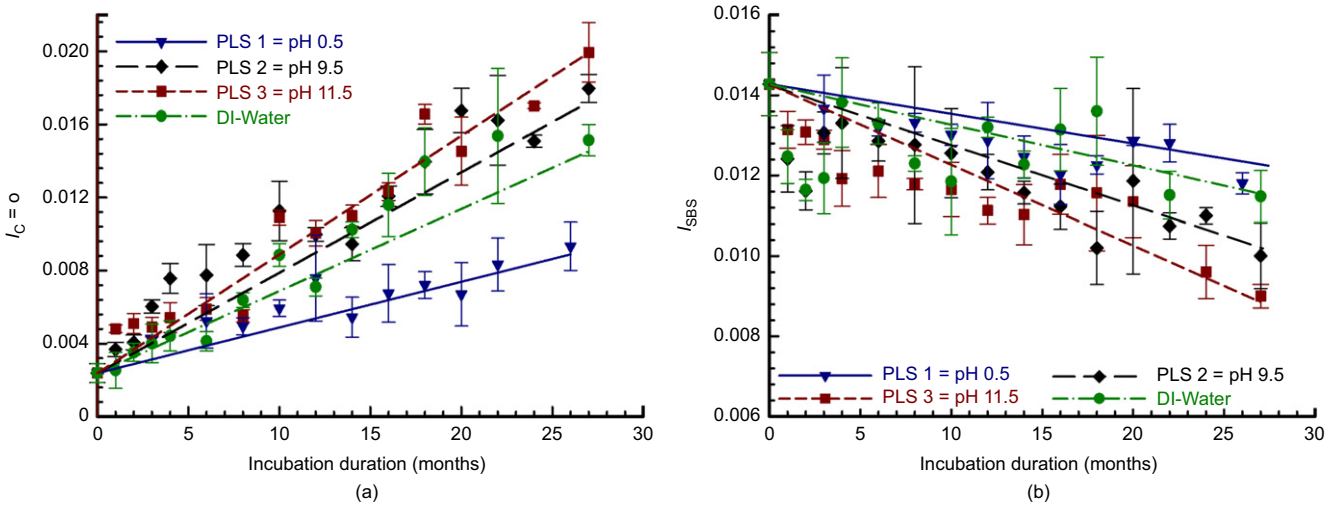

Figure 3. Variation of the $I_{C=O}$ and I_{SBS} with incubation time at 70°C in PLS1, PLS2, and PLS3: (a) $I_{C=O}$; (b) I_{SBS}. Data in DI-Water are from Samea and Abdelaal (2023)

PLS3, reaching 71% and 60% of the initial value, respectively, at the end of incubation, versus a 15% reduction in PLS1. However, the I_{SBS} data does not signify the effect of pH on the degradation of the SBS copolymer given the high scatter in the data at the different incubation durations in all the solutions examined. Overall, incubation in alkaline media and the neutral DI water resulted in more oxidative degradation of the bitumen coat than the low pH PLS1 while there was no clear effect of the pH on the degradation of the SBS copolymer.

3.2. Effect of pH on mechanical properties of BGM at 70°C

In all three solutions, the mechanical strengths (the maximum tensile stress and peak puncture force; Figures 4a and 4c) of the BGM samples were retained at the initial values for the first 4 months. Then, there was a gradual decrease with time until reaching constant values toward the end of the incubation. The fastest decrease in tensile strength was in PLS3 reaching 18% of the initial value after 13 months, then in PLS2 reaching the same value after 15 months, while the slowest decrease was in PLS1 also reaching 18% of the initial values but after 19 months (Figure 4a). Similar behaviour was observed for the puncture resistance in which the value decreased to 22% of the initial values after 13 months in PLS3, 14 months in PLS2, and 18 months in PLS1 (Figure 4c).

For the elongations at the maximum (peak) strength/force (ε_{max}), there was a gradual decrease in the values after incubation (i.e. there was no retention time) to reach constant values in all mining solutions (Figures 4b and 4d). In PLS1, ε_{max} from the tensile and puncture tests decreased to 12% and 50% of the initial value, after 21 and 16 months, respectively. In PLS2 and PLS3, the trend was similar to PLS1 since ε_{max} from both tests decreased to almost the same values as in PLS1, but the decrease was faster in PLS3 and PLS2 than in PLS1. Thus, similar to the tensile strength and puncture resistance, incubation in alkaline solutions (PLS2 and PLS3) showed higher degradation rates in tensile and puncture elongations at the maximum (peak) strength/force at 70°C than the acidic media (PLS1). Comparing the degradation in the mechanical properties in the mining solutions to those reported in DI water by Samea and Abdelaal (2023) for the same BGM shows that the degradation rates in DI water were slightly slower than in alkaline solutions but faster than those in the low pH solution. This shows that incubation in the acidic solution was the least aggressive media on the mechanical properties of the BGMs.

3.3. Discussion of BGM ageing mechanism in different mining solutions at elevated temperatures

Due to the exposure of the BGM to elevated temperatures, dissolved oxygen, and chemical constituents of the solutions at extreme pH, oxidative degradation of the BGM was observed in all mining solutions that resulted in changes in its chemical and rheological properties. The degradation of the BGM involved oxidation of the bitumen coat (increase in $I_{C=O}$), and chain scissioning of the SBS copolymer (decrease in I_{SBS}), that led to an increase in the bitumen rigidity (increase in G^* and decrease in δ) and crosslinking of the bitumen molecules (change in T_g). However, the degradation of these properties in all the mining solutions with different pHs was substantially lower than the degradation observed for the same BGM in air at 70°C that was examined by Samea and Abdelaal (2023). This implies that among all factors contributing to the degradation of the bitumen coat, air exposure (i.e. exposure to oxygen) has the highest effect on its oxidative degradation.

For the different aqueous solutions at 70°C, increasing the pH from 0.5 to 11.5 affected the degree of ageing of the bitumen coat. Based on a student's *t*-test analysis of the degradation in the different chemical and rheological properties at different incubation times, the difference in the degradation in these properties was statistically insignificant (at a 95% confidence level) in DI water and the two alkaline solutions (i.e. PLS2 and PLS3). However,

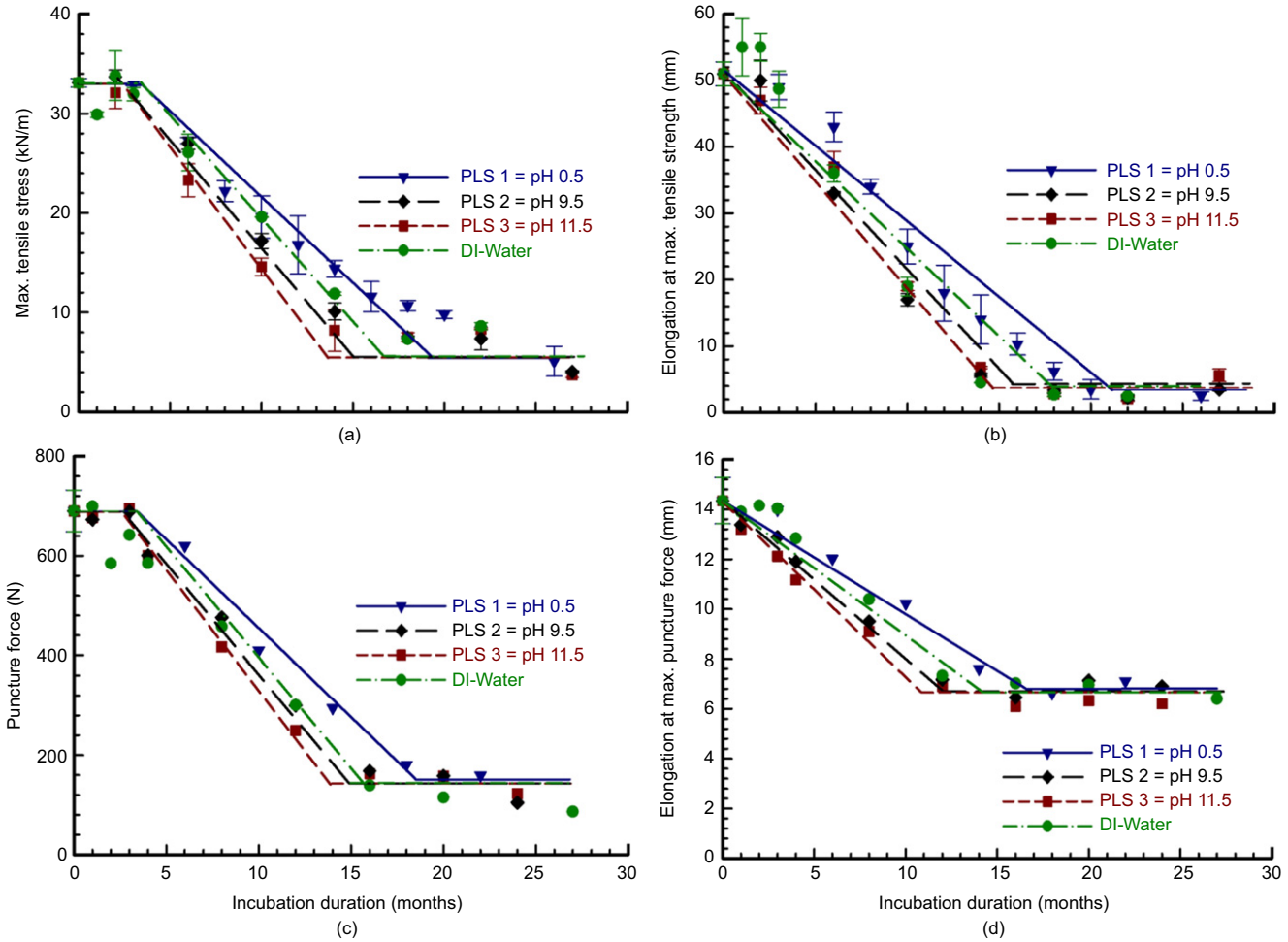

Figure 4. Variation in mechanical properties in the machine direction with incubation time at 70°C in DI-water, PLS1, PLS2, and PLS3: (a) maximum (peak) tensile stress; (b) elongation at (maximum) tensile strength; (c) maximum (peak) puncture force; (d) elongation at maximum puncture force. Error bars represent ±standard deviation of measured values. Data in DI-Water are from Samea and Abdelaal (2023)

the degradation obtained in the acidic PLS1 was slower (at a 95% confidence level) than in both the DI water and the alkaline solutions. This can be attributed to the formation of more oxygenated species with high molecular weight and polarity in the alkaline media and DI water (pH ≈ 6.5) than in the acidic media that increased the stiffness and rigidity of the bitumen (Pang *et al.* 2018; Wang *et al.* 2019b; Ding *et al.* 2022).

With such relatively low degradation in the bitumen coat in all mining solutions (relative to air ageing), the BGM exhibited degradation in its mechanical properties in the three mining solutions. This degradation in the mechanical properties of the BGM was similar to the degradation of the NW-GTX samples which were separately immersed in the three mining solutions at 70°C (Figure 5) and can be attributed to the hydrolysis of its polyester fibres (Samea and Abdelaal 2023). This shows that the chemical constituents of these solutions can interact with the coated and bitumen impregnated NW-GTX of the BGM and result in its degradation even with a slightly degraded bitumen coat (even in PLS1) and despite the effectiveness of sealing the edges of the BGM coupons (discussed in Section 2.3). This implies that, at elevated temperatures, the bitumen coat offered limited protection to the reinforcement layer in the mining solutions irrespective of their pHs, and resulted in the degradation in the mechanical properties of the BGM.

While the chemical constituents of all the solutions can interact with the NW-GTX of the aged BGM, the degradation rates of the mechanical properties of the BGM were faster in the alkaline solutions than in the low pH solution at 70°C (at the 90% confidence level). The faster degradation in mechanical properties of the BGM in the alkaline solutions can be attributed to the higher changes in the morphology and molecular weight of the polyester fibres in the alkaline media than in the acidic media (Nguyen-Tri *et al.* 2014). In this case, the rate of degradation in mechanical properties of the BGM depends on the resistance of the polyester NW-GTX to degradation, notwithstanding the subtle degradation of the bitumen coat. Overall, the degradation behaviour of the BGM in solutions with pH 0.5, 6.5 (i.e. DI water), 9.5, and 11.5 shows that the degradation of the BGM properties was slower in the low pH solution than in the DI water or the alkaline solutions examined. Additionally, increasing the pH from 6.5 to 11.5 resulted in a statistically insignificant increase

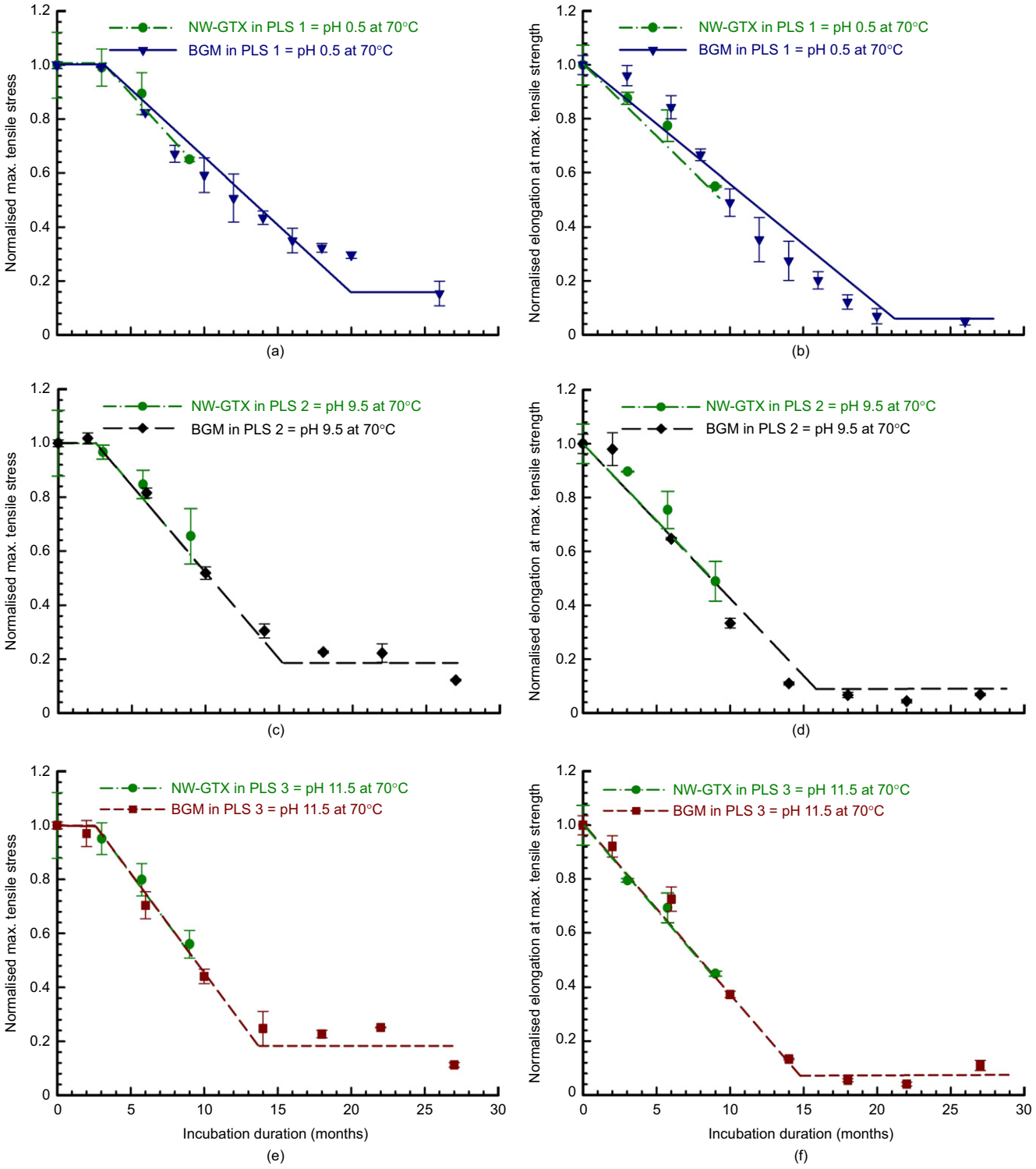

Figure 5. Variation in normalized (aged values/initial values) tensile properties of BGM Vs. NW-GTX at 70°C in the machine direction with incubation time for (a) maximum (peak) tensile stress in PLS1; (b) elongation at (maximum) tensile strength in PLS1; (c) maximum (peak) tensile stress in PLS2; (d) elongation at (maximum) tensile strength in PLS2; (e) maximum (peak) tensile stress in PLS3; (f) elongation at (maximum) tensile strength in PLS3

in the oxidative degradation of the bitumen coat and the degradation of the mechanical properties of the BGM.

3.4. Effect of incubation temperature on the different properties of the BGM

To establish the degradation rates in the different properties of the BGM, the coupons were incubated at 22, 40 and 55°C, in addition to the 70°C discussed in the previous sections. For the chemical and rheological properties of the BGM in PLS1 at temperatures below 70°C, oxidative degradation in the bitumen coat was only observed at 55°C based on the changes in the values of T_g, $I_{C=O}$ and I_{SBS} (Figure 6). However, the changes in the bitumen rigidity implied from the changes in G^* and δ

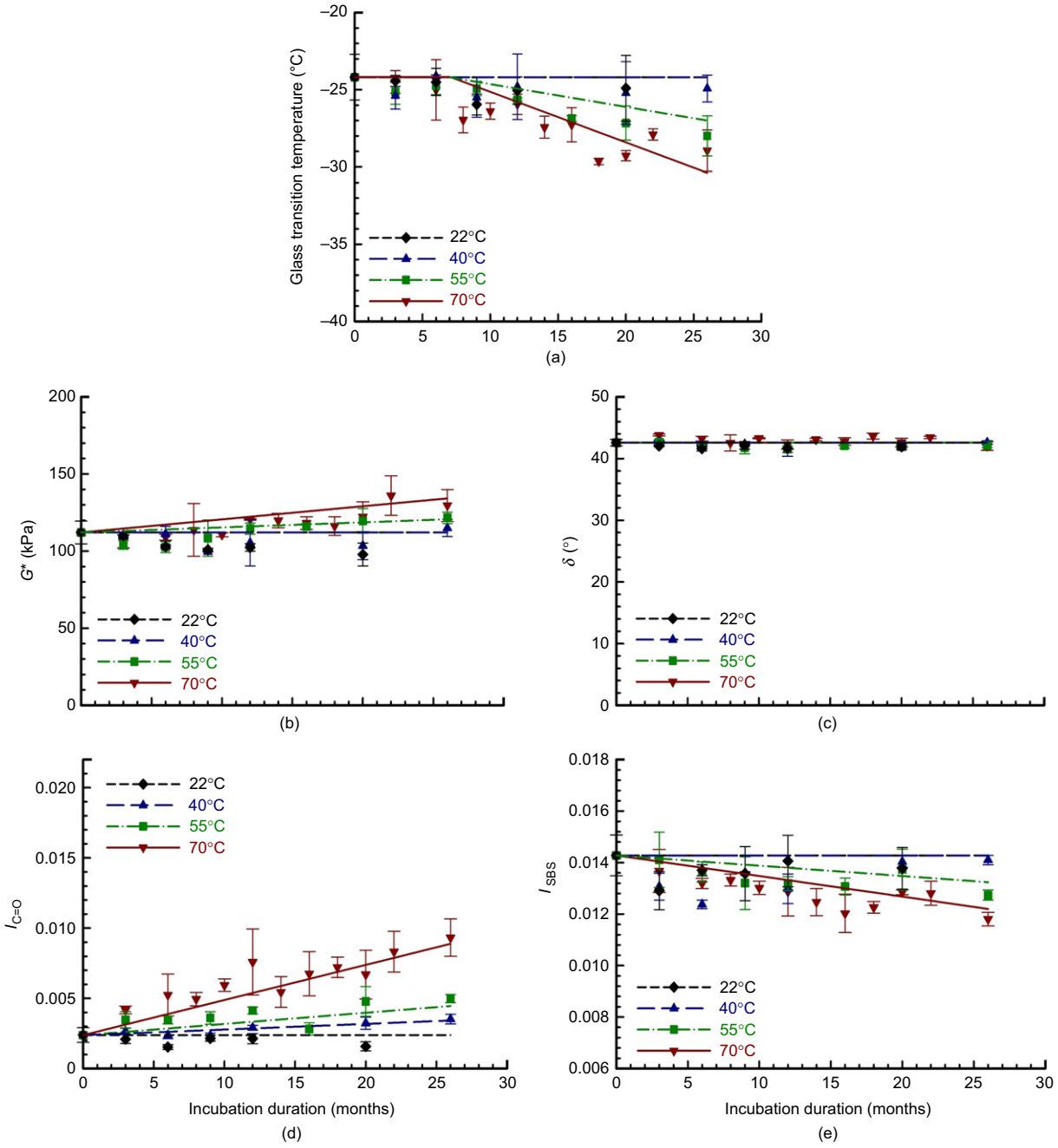

Figure 6. Variation in chemical and rheological properties with incubation time at different temperatures in PLS1 for (a) glass transition temperature; (b) complex shear modulus; (c) phase angle; (d) $I_{C=O}$; (e) I_{SBS}

were relatively low at all temperatures, including the 70°C. For PLS2 (Figure 7) and PLS3 (Figure 8), changes in the chemical structure of the bitumen obtained from the T_g, $I_{C=O}$ and I_{SBS} results were observed at all incubation temperatures except for 22°C. For the changes in the bitumen rigidity, there was a similar increase in G^* values at all incubation temperatures except for 22°C while changes in δ were only observed at 55 and 70°C. These results show that the changes in the bitumen rigidity in the three mining solutions took place after the oxidative degradation of the bitumen coat inferred from the changes in T_g, $I_{C=O}$ and I_{SBS}. The results of the chemical and rheological properties at different temperatures emphasize the higher resistance of the bitumen to the acidic solution than the alkaline solutions that showed degradation at temperatures as low as 40°C during the 26 months of incubation.

The effect of temperature on the mechanical properties was evaluated based on the tensile properties only given the smaller size of the samples relative to the puncture test. In all three incubation media, the decrease in tensile strength was only observed at 70°C, while at 55°C and lower temperatures, the strength was retained at the initial values during the 26 months of incubation (Figures 9a, 9c and 9e). For ε_{max}, degradation was observed at 55°C in all three mining solutions reaching 91, 82 and 74% of the initial values at the end of the incubation period in PLS1, PLS2 and PLS3, respectively (Figures 9c, 9d and 9f).

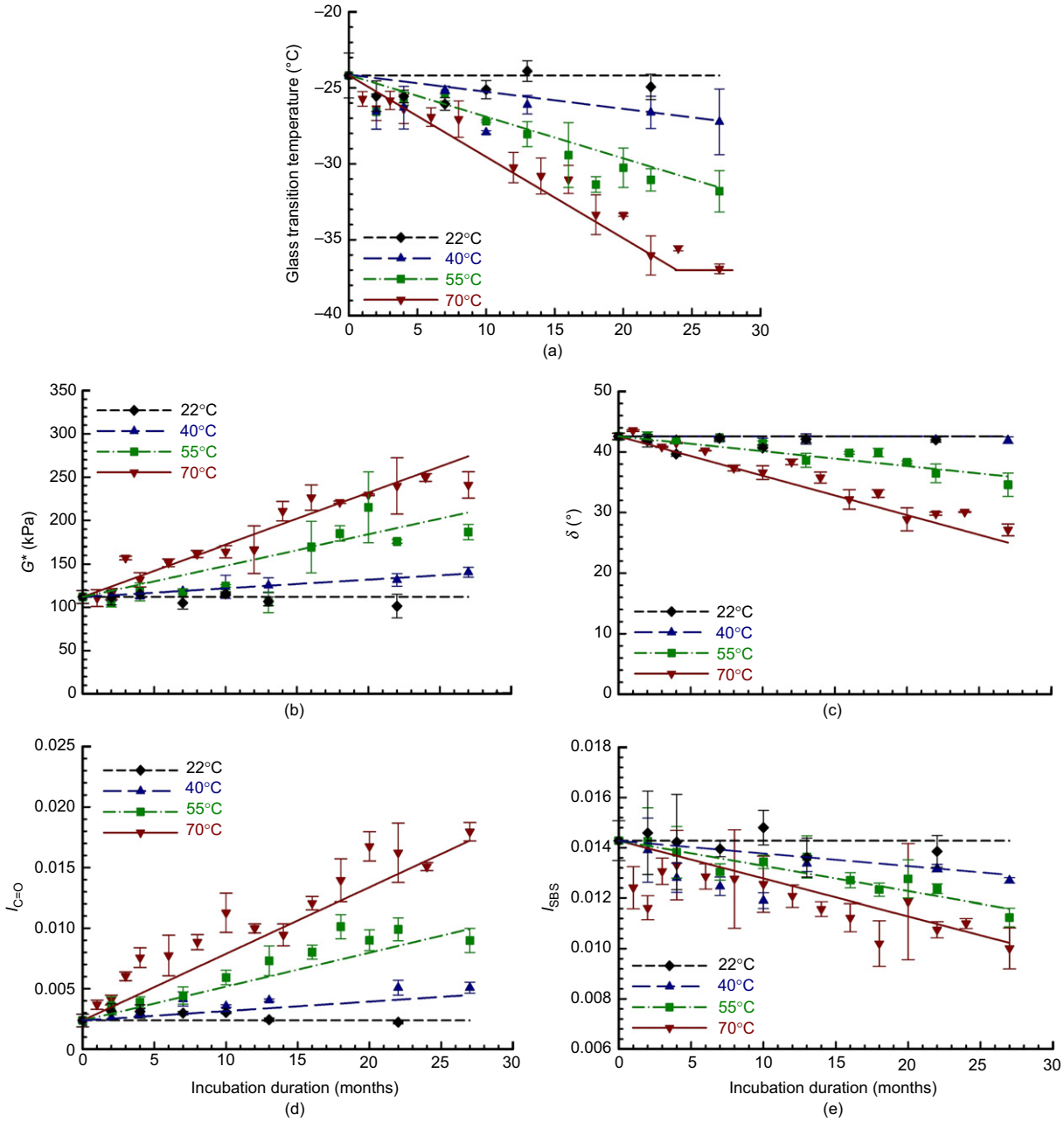

Figure 7. Variation in chemical and rheological properties with incubation time at different temperatures in PLS2 for (a) glass transition temperature; (b) complex shear modulus; (c) phase angle; (d) $I_{C=O}$; (e) I_{SBS}

The faster degradation of ε_{max} than the strength can be attributed to an increase in the bitumen rigidity at 55°C that affected the elongations but contributed to the retention of the tensile strength of the BGM (Samea and Abdelaal 2023). Overall, degradation in ε_{max} was faster in PLS3 and PLS2 than in PLS1 at 55°C, similar to the 70°C due to the higher changes in the G^* and δ in the high pH solutions than in the low pH solution.

3.5. Arrhenius modelling and nominal failure predictions

Nominal failure of the BGM as a liner material can be reached either when the BGM loses its mechanical properties or when the bitumen coat loses its viscoelastic characteristics (i.e. reaches brittleness). This is because, under field stresses, the BGM may rupture when degrading to such low mechanical resistance and hence lose its hydraulic barrier function. Likewise, the brittleness of the bitumen coat due to ageing may result in its cracking under field stresses. Although Samea and Abdelaal (2023) showed for a highly degraded bitumen coat that these cracks did not propagate with the full thickness of the BGM, it is expected that they could result in a reduction in the waterproofing characteristics of the BGM and the direct exposure of the reinforcement layers to the solution that could accelerate their degradation. Thus, Samea and Abdelaal (2023) proposed that time to nominal failure (t_{NF}) for BGMs can be established as the time taken for either a mechanical property to reach 50% of the minimum value specified by the manufacturer or the bitumen coat to reach brittleness.

For the mechanical properties, nominal failure was assessed based on the tensile ε_{max} since it showed faster

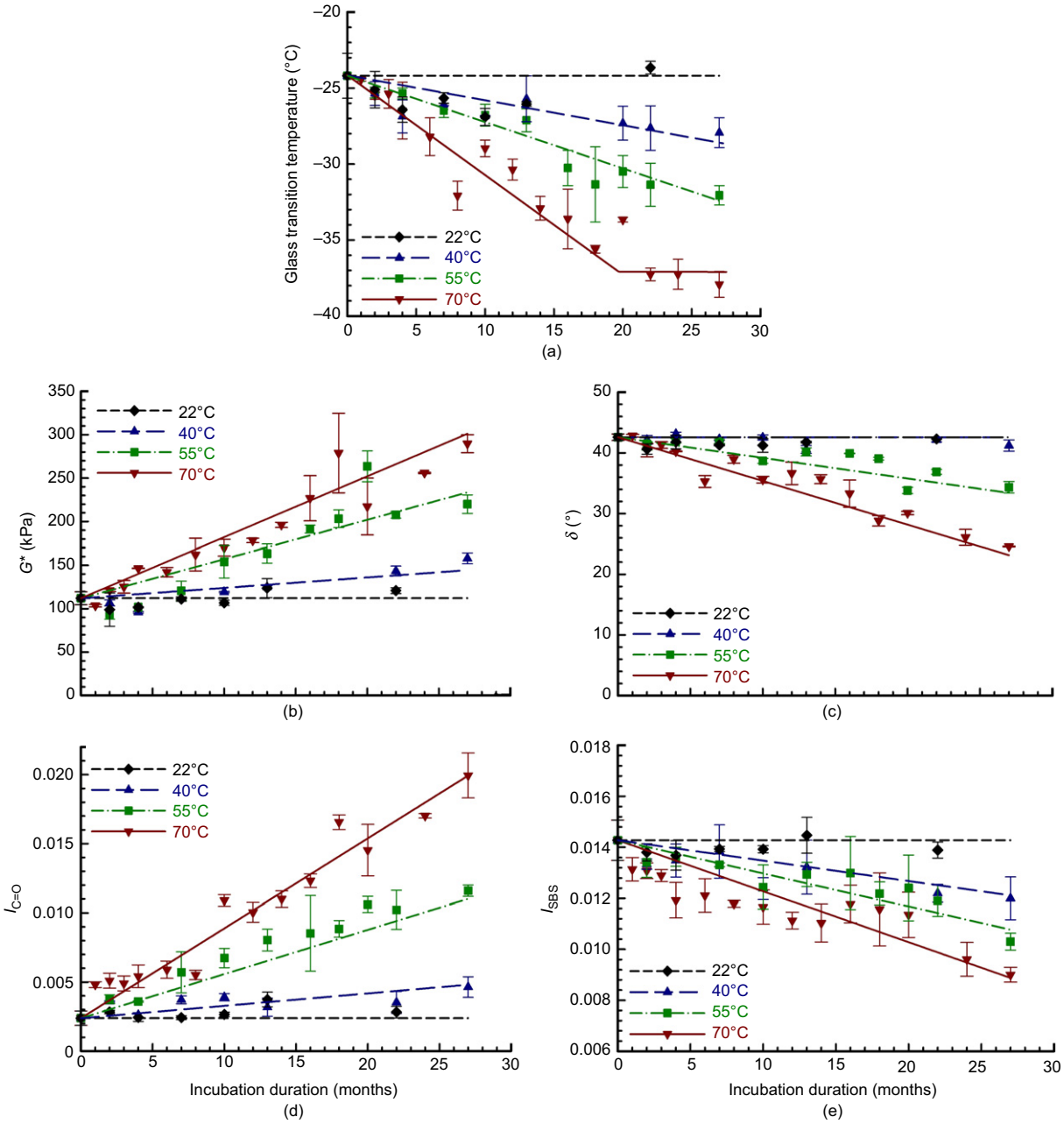

Figure 8. Variation in chemical and rheological properties with incubation time at different temperatures in PLS3 for (a) glass transition temperature; (b) complex shear modulus; (c) phase angle; (d) $I_{C=O}$; (e) I_{SBS}

degradation than the tensile strength and hence shall result in more conservative estimates of BGM degradation times. Additionally, the puncture ε_{max} was not used since the degradation in mechanical properties was assessed based only on the tensile properties at the different temperatures as discussed in Section 3.4. However, the results at 70°C show that the t_{NF} assessed based on the tensile ε_{max} reaching 50% of the minimum value specified by the manufacturer (i.e. 0.5 × 33 mm) was similar to the t_{NF} assessed based on the puncture ε_{max} reaching 50% of the initial value (Figures 4b and 4d). Thus, it is expected that these two index properties should result in the same estimates of the t_{NF} at the lower temperatures.

For the time to brittleness, the t_{NF} was assessed based on the chemical and rheological properties reaching the values measured at the time the BGM exhibited brittleness in the bitumen coat. According to Samea and Abdelaal (2023), when the same BGM was exposed to air at different temperatures, the measured values of G^*, δ and $I_{C=O}$ at the brittleness of the bitumen were 640 kPa, 20° and 0.035, respectively. Although in the current study these values were not reached by the end of the incubation time, the best fit lines (i.e. the degradation rates) established in the current study for these properties (Figures 6–8) were used to predict the time at which G^*, δ and $I_{C=O}$ reach these values at the different experimental temperatures.

The degradation rates obtained from the slope of degradation curves of ε_{max}, G^*, δ and $I_{C=O}$ at the different experimental temperatures in PLS1, PLS2, and PLS3 (Table 4) were used to extrapolate the degradation at lower field temperatures. This was done using Arrhenius modelling that was previously used in

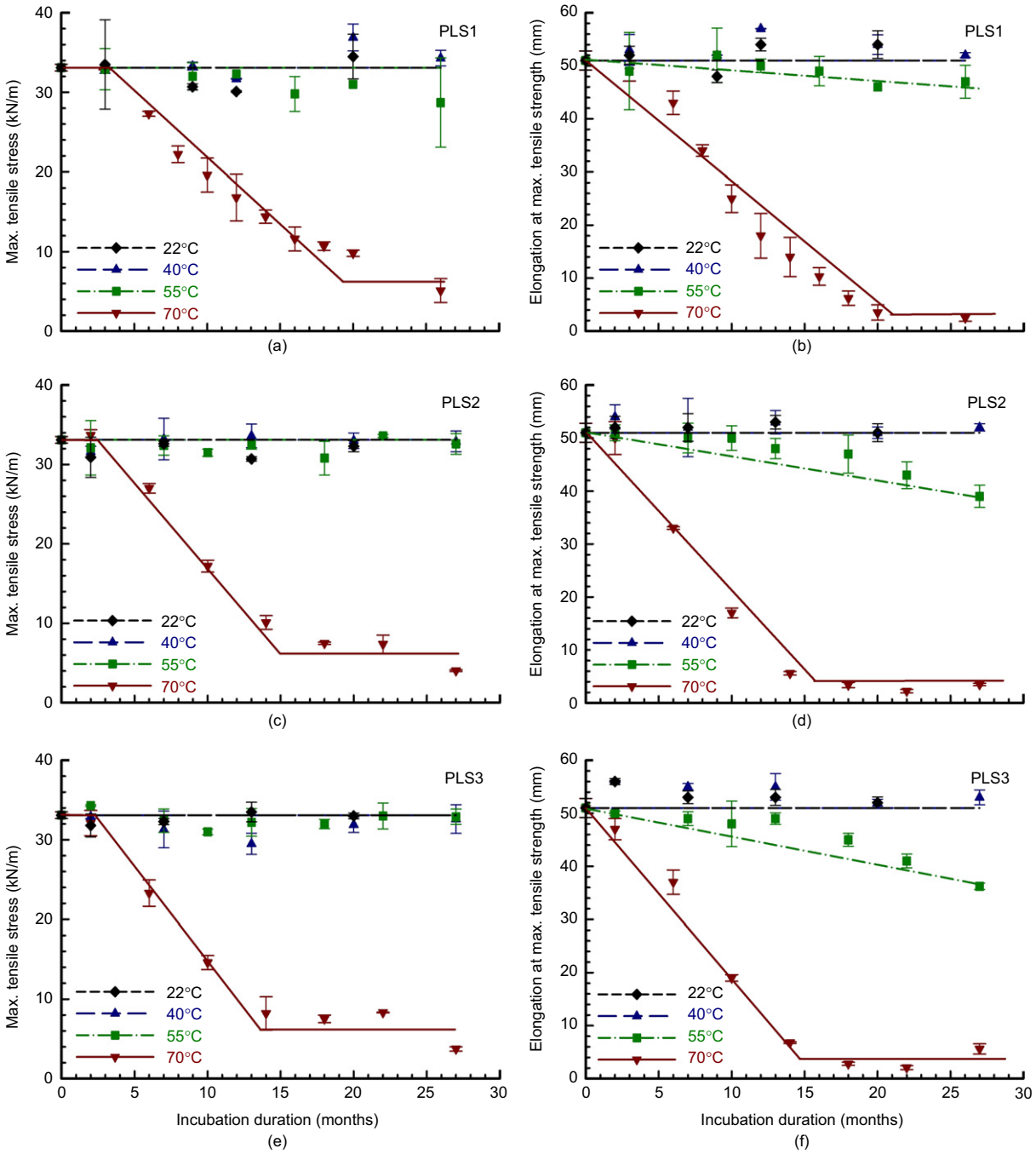

Figure 9. Variation in tensile properties in the machine direction with incubation time at different temperatures for (a) maximum (peak) tensile stress in PLS1; (b) elongation at (maximum) tensile strength in PLS1; (c) maximum (peak) tensile stress in PLS2; (d) elongation at (maximum) tensile strength in PLS2; (e) maximum (peak) tensile stress in PLS3; (f) elongation at (maximum) tensile strength in PLS3

polymer/geosynthetics and bitumen research (e.g. Koerner *et al.* 1992; Mastrofini and Scarsella 2000; Rek and Barjaktarović 2002; Lesueur 2009; Jin *et al.* 2011; Naskar *et al.* 2012; Wang *et al.* 2019b). The Arrhenius equation can be written as:

$$\ln(s) = \ln(A) - \left(\frac{E_a}{R}\right)\left(\frac{1}{T}\right) \quad (3)$$

where s, degradation rate (month^{-1}); T, absolute temperature (K); A, constant called a collision factor (month^{-1}); E_a, activation energy (J·mol^{-1}); $R = 8.314$ (J·mol^{-1}·K^{-1}) is the universal gas constant.

Different Arrhenius plots (Figure 10) were used to separately establish the degradation rates for the chemical and rheological properties related to the bituminous component and for the mechanical properties related to the geosynthetic component (i.e. NW-GTX). This is because Equation (3) cannot be used to predict the overall degradation in a multi-component material such as BGMs involving different reaction rates related to the different degradation mechanisms in its different components (Samea and Abdelaal 2023).

Based on the data available at the time of writing, the Arrhenius plots for ε_{max} (in all three solutions), δ (in PLS2

Table 4. Degradation rates of the BGM samples immersed in different mining solutions

Solution	Property	Degradation rates at different temperatures (month^{-1})			
		22°C	40°C	55°C	70°C
PLS1	ε_{max}	NR	NR	0.2	1.9
	G^*	NR	NR	0.33	0.85
	δ	NR	NR	NR	NR
	$I_{C=O}$	NR	0.00004	0.00008	0.00025
PLS2	ε_{max}	NR	NR	0.45	2.9
	G^*	NR	1	3.65	6
	δ	NR	NR	0.245	0.65
	$I_{C=O}$	NR	0.00008	0.00028	0.00055
PLS3	ε_{max}	NR	NR	0.55	3.2
	G^*	NR	1.2	4.5	7
	δ	NR	NR	0.34	0.72
	$I_{C=O}$	NR	0.00009	0.00032	0.00065
DI water[a]	ε_{max}	NR	NR	0.45	2.2
	G^*	NR	1	3.5	5
	δ	NR	NR	0.25	0.50
	$I_{C=O}$	NR	0.000068	0.00025	0.00045

NR = Degradation in properties was not reached during the current study.
[a]Data in DI-Water are from Samea and Abdelaal (2023).

and 3) and G^* (in PLS1) were established based on two temperatures only. Since Arrhenius plots established based only on two elevated temperatures are approximate and could result in shorter predictions at lower temperatures (i.e. conservative), the activation energies (i.e. the slopes of the Arrhenius plots) were assumed to be similar to the values reported in Samea and Abdelaal (2023) until more data become available. These activation energies were established for the same properties of the same BGM when immersed in the air based on three or more elevated temperatures. This assumption resulted in a coefficient of determination (R^2) < 1 for all three properties (as indicated in Figure 10) despite having two data points for the Arrhenius plots. For G^* (in PLS2 and 3) and $I_{C=O}$, the Arrhenius plots were established based on three temperatures, and hence the best fit line gave R^2 greater than 0.95 with a range of activation energies that varied from 54 to 57 kJ·mol^{-1}.

The estimated t_{NF} of the BGM in the three PLS is shown in Table 5 for different field temperatures between 5 and 85°C. In general, the t_{NF} based on ε_{max} (i.e. values reaching 50% of the minimum value specified by the BGM manufacturer) was shorter than the predictions based on the time to the brittleness of bitumen coat (i.e. G^*, δ and $I_{C=O}$ reaching the values at brittleness) in all mining solutions at different temperatures. For example, in PLS2 at 10°C t_{NF} was 130, 350, 300, and 320 years, based on ε_{max}, G^*, δ and $I_{C=O}$, respectively. For the t_{NF} based on ε_{max} in different solutions, the predictions at 10°C were 230, 130, and 110 years, for PLS1, PLS2 and PLS3, respectively. For the t_{NF} at the same temperature based on the brittleness in the bitumen coat, the shortest predictions among G^*, δ and $I_{C=O}$ were 670 years in PLS1, 300 years in PLS2, and 230 years in PLS3. Thus, based on the different nominal failure criteria, the predictions established based on the current data show substantially better durability of the BGM in low pH solutions than in high pH at low field temperatures.

3.6. Implications for the time to nominal failure of BGMs in heap leach pads

While the design life of heap leaching operations is typically around 10 years (Breitenbach 2005; Ghorbani *et al.* 2016), some facilities have been operating for more than 20 years with several leaching cycles (Breul *et al.* 2008; Lupo 2010). With such a relatively short design life (relative to waste containment applications), heap leaching operations may require temperatures at or above 50°C to maximize the metal recovery (Thiel and Smith 2004; McBride *et al.* 2018). However, higher (>70°C) and lower (<10°C) temperatures were also reported for some heap leaching applications (Breul *et al.* 2008; Steemson and Smith 2009; Abdelaal *et al.* 2011; Sinho and Smith 2015). Given such variation in the heap leaching operating temperatures, the predictions reported in Table 5 highlight the need for considering the expected liner temperature when selecting BGMs for the primary liner material to meet the required design life of heap leach pads. For a low-temperature application (e.g. at 10°C), both high pH and low pH solutions gave predictions greater than 100 years based on the different nominal failure criteria of the BGM. Hence, at such low liner temperatures, BGMs could be suitable for long leaching cycles or long design lives. At a liner temperature of 50°C, predictions based on the degradation in the mechanical properties (i.e. ε_{max}) were less than the typical design life of heap leach pads of 10 years for the three examined solutions with different pHs. However, the average nominal failure of the BGM based on the time to brittleness of the bitumen coat (i.e. the average of the predictions based on G^*, δ and, $I_{C=O}$) that can potentially affect its water tightness was 118 years for PLS1, 15 years for PLS2, and 13 years for PLS3. This shows that if the tensile strains in the field were limited to the values that do not induce long-term ruptures in the aged BGM with such low mechanical resistance (e.g. using thick protection layers to limit gravel indentations), the BGM

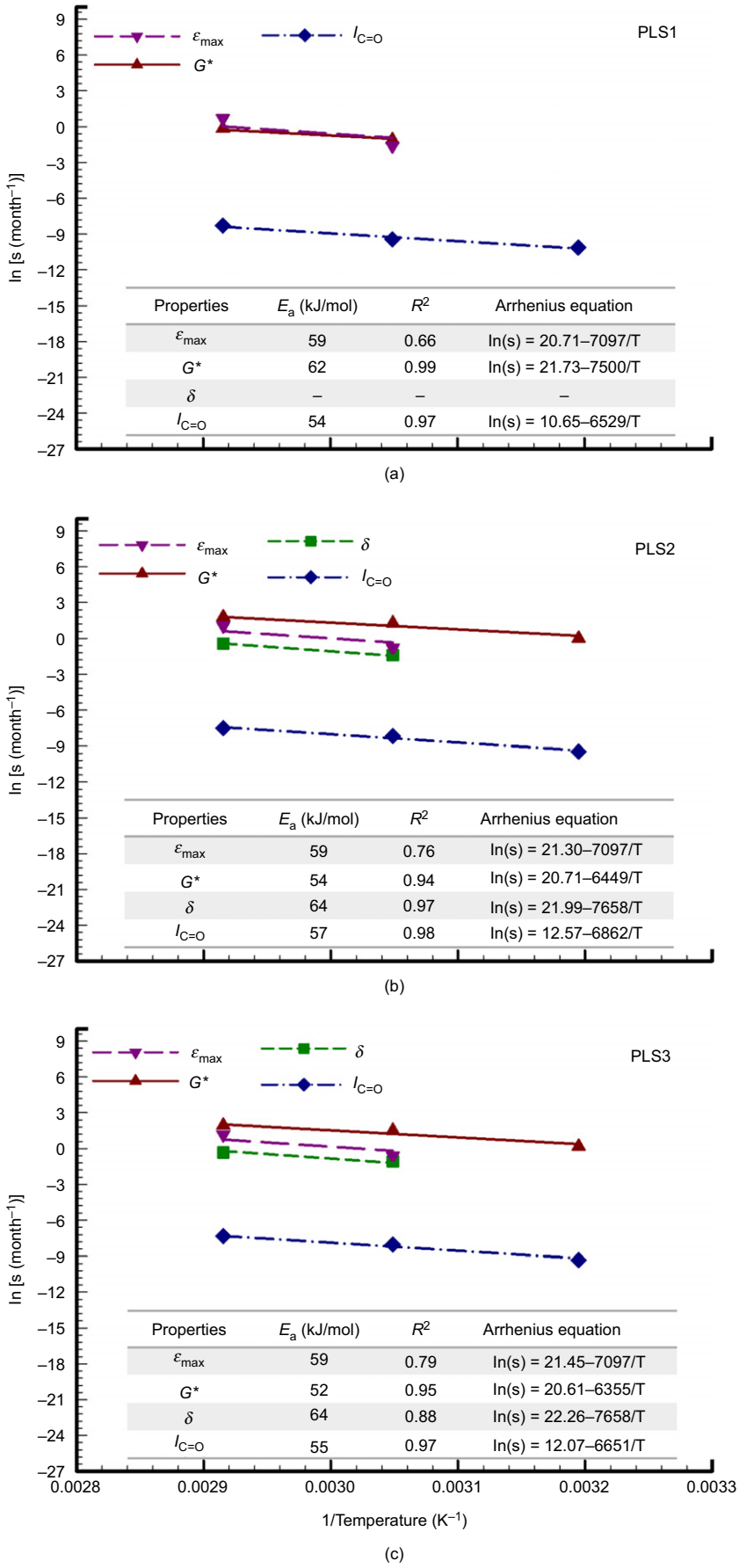

Figure 10. Arrhenius plots of the elongation at (maximum) tensile strength (ε_{max}), complex shear modulus (G^*), phase angle (δ), and carbonyl index ($I_{C=O}$) for the samples immersed in (a) PLS1; (b) PLS2; (c) PLS3 (based on data collected at 22, 40, 55, and 70°C)

Table 5. Predicted time to nominal failure (t_{NF}) of the BGM samples immersed in the different mining solutions in years (rounded to two significant digits)

T (°C)	t_{NF} (Years)											
	PLS1				PLS2				PLS3			
	ε_{max}	G^*	δ	$I_{C=O}$	ε_{max}	G^*	δ	$I_{C=O}$	ε_{max}	G^*	δ	$I_{C=O}$
5	360	>1000	—	>1000	200	530	480	495	170	420	370	380
10	230	>1000	—	670	130	350	300	320	110	280	230	250
20	100	>1000	—	310	55	160	120	140	45	130	90	110
30	45	900	—	150	25	80	50	65	20	65	40	55
40	20	400	—	75	11	40	22	30	9.7	35	17	25
50	10	195	—	40	5.6	20	10	16	4.8	17	8	13
55	7.2	135	—	30	4.0	15	7.2	11	3.5	12	5.6	10
70	2.8	50	—	12	1.6	6.5	2.6	4.6	1.3	5.5	2	4.1
85	1.2	20	—	5.4	0.7	3.0	1.1	2	0.6	2.5	0.8	1.8

Numbers in bold show the property governing the time to nominal failure.
For ε_{max}, time to nominal failure was established based on the time to reach 50% of the minimum value specified by the manufacturer.
For G^*, δ, and $I_{C=O}$, time to nominal failure was established based on the time to the brittleness of the bitumen coat when the values reach 620 kPa, 20°, and 0.035, respectively.

may meet the typical design life of heap leach pads of 10 years without losing its hydraulic barrier function.

The predicted t_{NF} given in Table 5 is for the BGM immersed in synthetic mining solutions. It has been shown that degradation times are substantially longer in a composite liner than in the double-sided immersion that was used in the experiments discussed herein (e.g. Rowe and Rimal 2008; Rowe *et al*. 2013). Thus, while the predictions presented are considered conservative estimates of nominal failure, they should not be considered as the service life of the BGM in the field since the stresses on the liner were not simulated in the immersion tests. However, these predictions show superior chemical durability of BGMs in acidic solutions than in alkaline solutions. Additionally, they highlight the need for limiting the tensile strains in the field in high stress applications due to the relatively fast degradation in the mechanical properties of the BGM than the chemical and rheological properties, especially at elevated temperatures.

4. SUMMARY AND CONCLUSIONS

The effect of incubation in solutions simulating low and high pH mining applications on the degradation behaviour of a 4.8 mm thick elastomeric BGM was investigated at four different temperatures (22, 40, 55, and 70°C) using oven immersion tests. The low pH (PLS1pH 0.5) stimulates the PLS found in copper, uranium, and nickel heap leaching while the two high pH (PLS2pH 9.5 and PLS3pH 11.5) solutions simulate the range of pHs and chemistries of gold and silver heap leaching. Tensile and puncture tests were used to characterize the degradation behaviour of the BGM reinforcement layers, while the rheological and chemical properties of the bitumen coat were assessed using MDSC, DSR and FTIR. For the BGM and conditions examined herein, the following conclusions were reached:

(*a*) Exposure to aqueous solutions at elevated temperatures resulted in faster degradation in the mechanical properties of the BGM than the degradation in rheological and chemical properties of the bitumen coat. This was attributed to the faster degradation of the NW-GTX by hydrolysis in the high or low pH mining solutions than the oxidative degradation of the bitumen coat.

(*b*) The degradation in both the bitumen coat and the mechanical properties of the BGM in the different mining solutions was slower in PLS1pH 0.5 than in DI water, PLS2, and PLS3 with pH 6.5, 9.5 and 11.5, respectively. Thus, the examined SBS modified BGM had higher resistance to degradation in acidic environments than neutral and alkaline media.

(*c*) Increasing the pH from 6.5 (DI water) to 9.5 and 11.5 (PLS2 and PLS3) resulted in a statistically insignificant increase in the degradation of the chemical, rheological and mechanical properties of the BGM. This shows that increasing the pH within this range had a slight effect on the degradation of the bitumen coat and the NW-GTX reinforcement layer.

(*d*) The degradation in the mechanical properties of the NW-GTX that was used in the manufacturing of the BGM and separately immersed in the three mining solutions was similar to the degradation of the BGM. Thus, even with the relatively low degradation in the bitumen coat at early incubation times and sealing the edges of the coupons, the solutions interacted with the coated and bitumen impregnated NW-GTX of the BGM resulting in its degradation.

(*e*) Predictions of the time to nominal failure of the BGM at typical heap leaching field temperatures between 10 and 50°C based on the degradation in the tensile elongation ranged from 230 to 10 years in

PLS1, 130 to 5.6 years in PLS2, and 110 to 4.8 years in PLS3. The average time to brittleness based on the different rheological and chemical properties ranged from 835 to 120 years in PLS1, 325 to 15 years in PLS2, and 255 to 13 years in PLS3. Although these predictions show the higher resistance of the BGM to the acidic solution than alkaline solutions, they highlight the significant effect of elevated temperatures on the long-term performance of BGMs in all the solutions examined.

(*f*) To ensure better long-term performance of the BGMs in heap leaching applications, the long-term tensile strains in the BGMs should be limited due to the relatively fast degradation in the mechanical properties of the BGM than the chemical and rheological properties, especially at elevated temperatures. In this case, the time to brittleness is expected to govern the nominal failure of the BGM in the field in the different mining solutions before losing its hydraulic barrier function.

This study presented insights into the long-term performance of a particular elastomeric BGM in simulated heap leaching solutions. The experiments only involved the double-sided exposure of the BGM to solutions without the application of any stresses. While they present aggressive chemical exposure conditions relative to the single-sided exposure in the field (Rowe and Rimal 2008), the service life of the BGM in the field (i.e. loss of the hydraulic barrier function) can be shorter or longer than the predictions presented herein. This is because the service life of the GMB depends on the magnitude of the long-term stresses and strains in the field and whether they can induce ruptures in the liner at such low resistance of the GMB after degradation (Rowe *et al*. 2013; Abdelaal *et al*. 2014).

ACKNOWLEDGEMENTS

The research presented in this paper was funded by Titan Environmental Containment Ltd. and the Natural Science and Engineering Research Council of Canada (NSERC) through the Collaborative Research and Development program. The used equipment were provided through funding from the Canada Foundation for Innovation (CFI) and the Ontario Ministry of Research and Innovation.

NOTATION

Basic SI units are shown in parentheses.

δ	phase angle (°)
ε_{max}	elongation at the maximum (peak) strength/force (mm)
G^*	complex shear modulus (Pa)
$I_{C=O}$	carbonyl index (dimensionless)
I_{SBS}	butadiene index (dimensionless)
T_g	glass transition temperature (°C)

ABBREVIATIONS

ASTM	American Society for Testing and Materials
BGM	bituminous geomembranes
DI	deionized
DSR	dynamic shear rheometer
FTIR	Fourier transform infrared spectroscopy
GMB	geomembranes
LVE	linear viscoelastic
MDSC	modulated differential scanning calorimetry
NW-GTX	nonwoven polyester geotextile
PLS	pregnant leach solution
RCS	refrigerated cooling system
SBS	styrene-butadiene-styrene

REFERENCES

Abdelaal, F. B. & Rowe, R. K. (2017). Effect of high pH found in low-level radioactive waste leachates on the antioxidant depletion of a HDPE geomembrane. *Journal of Hazardous, Toxic, and Radioactive Waste*, **21**, No. 1, https://doi.org/10.1061/(ASCE)HZ.2153-5515.0000262.

Abdelaal, F. B. & Rowe, R. K. (2023). Physical and mechanical performance of a HDPE geomembrane in ten mining solutions with different pHs. *Canadian Geotechnical Journal*, https://doi.org/10.1139/cgj-2022-0419.

Abdelaal, F. B., Rowe, R. K., Smith, M. & Thiel, R. (2011). OIT Depletion in HDPE geomembranes used in contact with solutions having very high and low pH. *Proceedings of the 14th Pan-American Conference of Soil Mechanics and Geotechnical Engineering*, Pan-Am CGS 2011 Organizing Committee, Toronto, ON, Canada, 7p.

Abdelaal, F. B., Rowe, R. K. & Brachman, R. W. I. (2014). Brittle rupture of an aged HPDE geomembrane at local gravel indentations under simulated field conditions. *Geosynthetics International*, **21**, No. 1, 1–23, https://doi.org/10.1680/gein.13.00031.

Aguiar-Moya, J. P., Salazar-Delgado, J., García, A., Baldi-Sevilla, A., Bonilla-Mora, V. & Loría-Salazar, L. G. (2017). Effect of ageing on micromechanical properties of bitumen by means of atomic force microscopy. *Road Materials and Pavement Design*, **18**, No. sup2, 203–215, https://doi.org/10.1080/14680629.2017.1304249.

Airey, G. (2003). Rheological properties of styrene butadiene styrene polymer modified road bitumens. *Fuel*, **82**, No. 14, 1709–1719, https://doi.org/10.1016/S0016-2361(03)00146-7.

Ali, A. H., Mashaan, N. S. & Karim, M. R. (2013). Investigations of physical and rheological properties of aged rubberised bitumen. *Advances in Materials Science and Engineering*, **2013**, 239036, 7 pages, https://doi.org/10.1155/2013/239036.

ASTM D4833/D4833M: *Standard Test Method for Index Puncture Resistance of Geomembranes and Related Products.* ASTM International, West Conshohocken, PA, USA.

ASTM D5035: *Standard Test Method for Breaking Force and Elongation of Textile Fabrics (Strip Method).* ASTM International, West Conshohocken, PA, USA.

ASTM D5199: *Standard Test Method for Measuring the Nominal Thickness of Geosynthetics.* ASTM International, West Conshohocken, PA, USA.

ASTM D5261: *Standard Test Method for Measuring Mass per Unit Area of Geotextiles.* ASTM International, West Conshohocken, PA, USA.

ASTM D7275: *Standard Test Method for Tensile Properties of Bituminous Geomembranes (BGM).* ASTM International, West Conshohocken, PA, USA.

ASTM E2602: *Standard Test Methods for the Assignment of the Glass Transition Temperature by Modulated Temperature Differential Scanning Calorimetry.* ASTM International, West Conshohocken, PA, USA.

Breitenbach, A. J. (2005). *Heap Leach Pad Design and Construction Practices in the 21st Century*, Vector Colorado LLC, pp. 1–9.

Breitenbach, A. J. & Thiel, R. (2005). A tale of two conditions: heap leach pad versus landfill liner strengths. In *Proceedings of GRI-19, December 2005*, Las Vegas, NV, USA, North American Geosynthetics Society (NAGS) – Geosynthetic Institute (GSI) Conference, 14e16.

Breul, B., Huru, M. & Palolahti, A. (2008). Use of bituminous geomembrane (BGM) liner for agnico eagle mine in Kittila (Finland). *Proceedings of the 4th European Geosynthetics Conference, Paper 245*, International Geosynthetics Society, Scotland, 8p.

Daly, N. & Breul, B. (2017). Exceptional longevity of bituminous geomembrane through several decades of practice. *Proceedings of 70th Canadian Geotechnical Conference*, Canadian Geotechnical Society (CGS), Ottawa, ON, Canada, 6p.

De Sá Araujo, M. D. F. A., Lins, V. D. F. C., Pasa, V. M. D. & Leite, L. F. M. (2013). Weathering aging of modified asphalt binders. *Fuel Processing Technology*, **115**, 19–25, https://doi.org/10.1016/j.fuproc.2013.03.029.

Ding, Y., Li, D., Zhang, H., Deng, M., Mao, X. & Cao, X. (2022). Investigation of aging behavior of asphalt under multiple environmental conditions. *Journal of Materials in Civil Engineering*, **34**, No. 3, https://doi.org/10.1061/(ASCE)MT.1943-5533.0004048.

Esford, F. & Janssens, G. (2014). Laboratory test results on a bituminous liner exposed to a weak acidic solution. *Proceedings of Geosynthetics Mining Solutions*, InfoMine, Vancouver, BC, Canada, p. 10.

Ewais, A. M. R., Rowe, R. K. & Scheirs, J. (2014). Degradation behaviour of HDPE geomembranes with high and low initial high-pressure oxidative induction time. *Geotextiles and Geomembranes*, **42**, No. 2, 111–126, https://doi.org/10.1016/j.geotexmem.2014.01.004.

Feng, B., Wang, H., Li, S., Ji, K., Li, L. & Xiong, R. (2022). The durability of asphalt mixture with the action of salt erosion: a review. *Construction and Building Materials*, **315**, 125749, https://doi.org/10.1016/j.conbuildmat.2021.125749.

Gao, Y., Gu, F. & Zhao, Y. (2013). Thermal oxidative aging characterization of SBS modified asphalt. *Journal of Wuhan University of Technology-Materials Science Edition*, **28**, No. 1, 88–91, https://doi.org/10.1007/s11595-013-0646-0.

Ghorbani, Y., Franzidis, J. P. & Petersen, J. (2016). Heap leaching technology – current state, innovations, and future directions: a review. *Mineral Processing and Extractive Metallurgy Review*, **37**, No. 2, 73–119, https://doi.org/10.1080/08827508.2015.1115990.

Gulec, S., Edil, T. & Benson, C. (2004). Effect of acidic mine drainage on the polymer properties of an HDPE geomembrane. *Geosynthetics International*, **2**, No. 11, 60–72, https://doi.org/10.1680/gein.2004.11.2.60.

Hsuan, Y. & Koerner, R. (1998). Antioxidant depletion lifetime in high density polyethylene geomembranes. *ASCE Journal of Geotechnical and Geoenvironmental Engineering*, **124**, No. 6, 532–541, https://doi.org/10.1061/(ASCE)1090-0241(1998)124:6(532).

Hung, A. M., Goodwin, A. & Fini, E. H. (2017). Effects of water exposure on bitumen surface microstructure. *Construction and Building Materials*, **135**, 682–688, https://doi.org/10.1016/j.conbuildmat.2017.01.002.

Jin, X., Han, R., Cui, Y. & Glover, C. J. (2011). Fast-rate–constant-rate oxidation kinetics model for asphalt binders. *Industrial & Engineering Chemistry Research*, **50**, No. 23, 13373–13379, https://doi.org/10.1021/ie201275q.

John, L. W. (2011). The art of heap leaching – the fundamentals.. In *International Conference on Percolation Leaching: The Status Globally and in Southern Africa*. Southern African Institute of Mining and Metallurgy, Misty Hills, Muldersdrift, South Africa, pp. 17–42.

Kaya, D., Topal, A., Gupta, J. & Mcnally, T. (2020). Aging effects on the composition and thermal properties of styrene-butadiene-styrene (SBS) modified bitumen. *Construction and Building Materials*, **235**, 117450–117457, https://doi.org/10.1016/j.conbuildmat.2019.117450.

Koerner, R. M., Lord, A. E. & Hsuan, Y. H. (1992). Arrhenius modeling to predict geosynthetic degradation. *Geotextiles and Geomembranes*, **11**, No. 2, 151–183, https://doi.org/10.1016/0266-1144(92)90042-9.

Kriz, P., Stastna, J. & Zanzotto, L. (2007). Effect of low-temperature isothermal conditioning on glass transition in asphalt binders. *Proceedings of the 52nd Annual Conference of the Canadian Technical Asphalt Association*, Niagra Falls, ON, Canada, vol. 52, pp. 159–184.

Lamontagne, J., Dumas, P., Mouillet, V. & Kister, J. (2001). Comparison by Fourier transform infrared (FTIR) spectroscopy of different ageing techniques: application to road bitumens. *Fuel*, **80**, No. 4, 483–488, https://doi.org/10.1016/S0016-2361(00)00121-6.

Lazaro, J. & Breul, B. (2014). Bituminous geomembrane in heap leach pads. *Proceedings of Heap Leach Solutions*, van Zyl, D. & Galindo, I. G., Editors, InfoMine, Lima, Peru, pp. 291–303.

Lesueur, D. (2009). The colloidal structure of bitumen: consequences on the rheology and on the mechanisms of bitumen modification. *Advances in colloid and interface science*, **145**, No. 1–2, 42–82, https://doi.org/10.1016/j.cis.2008.08.011.

Lu, X. & Isacsson, U. (1999). Chemical and rheological characteristics of styrene-butadiene-styrene polymer-modified bitumens. *Transportation research record*, **1661**, No. 1, 83–92, https://doi.org/10.3141/1661-13.

Lu, X., Talon, Y. & Redelius, P. (2008). Ageing of bituminous binders – laboratory tests and field data. In *Proceedings of the 4th Eurasphalt & Eurobitume Congress*, Copenhagen. Copenhagen, pp. 21–23.

Lupo, J. F. (2010). Liner system design for heap leach pads. *Geotextiles and Geomembranes*, **28**, No. 2, 163–173, https://doi.org/10.1016/j.geotexmem.2009.10.006.

Ma, T., Huang, X. M., Mahmoud, E. & Garibaldy, E. (2011). Effect of moisture on the aging behavior of asphalt binder. *International Journal of Minerals, Metallurgy, and Materials*, **18**, No. 4, 460–466, https://doi.org/10.1007/s12613-011-0463-4.

Masson, J. F. & Polomark, G. M. (2001). Bitumen microstructure by modulated differential scanning calorimetry. *Thermochimica Acta*, **374**, No. 2, 105–114, https://doi.org/10.1016/S0040-6031(01)00478-6.

Mastrofini, D. & Scarsella, M. (2000). The application of rheology to the evaluation of bitumen ageing. *Fuel*, **79**, No. 9, 1005–1015, https://doi.org/10.1016/S0016-2361(99)00244-6.

Mcbride, D., Gebhardt, J., Croft, N. & Cross, M. (2018). Heap leaching: modelling and forecasting using CFD technology. *Minerals*, **8**, No. 1, 9, https://doi.org/10.3390/min8010009.

Morsy, M. S. & Rowe, R. K. (2017). Performance of blended polyolefin geomembrane in various incubation media based on Std-OIT. In *Geotechnical Frontiers*, ASCE, Reston, VA, USA, pp. 1–10, https://doi.org/10.1061/9780784480434.001.

Morsy, M. S., Rowe, R. K. & Abdelaal, F. B. (2020). Longevity of 12 geomembranes in chlorinated water. *Canadian Geotechnical Journal*, **58**, No. 4, 479–495, https://doi.org/10.1139/cgj-2019-0520.

Müller, W. & Jacob, I. (2003). Oxidative resistance of high density polyethylene geomembranes. *Polymer Degradation and Stability*, **79**, No. 1, 161–172, https://doi.org/10.1016/S0141-3910(02)00269-0.

Naskar, M., Reddy, K. S., Chaki, T. K., Divya, M. K. & Deshpande, A. P. (2012). Effect of ageing on different modified bituminous binders: comparison between RTFOT and radiation ageing. *Materials and Structures*, **46**, No. 7, 1227–1241, https://doi.org/10.1617/s11527-012-9966-3.

Nguyen-Tri, P., El Aidani, R., Leborgne, É., Pham, T. & Vu-Khanh, T. (2014). Chemical ageing of a polyester nonwoven membrane used in aerosol and drainage filter. *Polymer Degradation and Stability*, **101**, 71–80, https://doi.org/10.1016/j.polymdegradstab.2014.01.001.

Pang, L., Zhang, X., Wu, S., Ye, Y. & Li, Y. (2018). Influence of water solute exposure on the chemical evolution and rheological properties of asphalt. *Materials (Basel)*, **11**, No. 6, 983, https://doi.org/10.3390/ma11060983.

Peggs, I. (2008). Prefabricated bituminous geomembrane: a candidate for exposed geomembrane caps for landfill closures. *Proceedings, The First Pan American Geosynthetics Conference and Exhibition*, IFAI, Roseville, MN, USA, pp. 191–197.

Petersen, J. (2016). Heap leaching as a key technology for recovery of values from low-grade ores–a brief overview. *Hydrometallurgy*, **165**, 206–212, https://doi.org/10.1016/j.hydromet.2015.09.001.

Rek, V. & Barjaktarović, Z. M. (2002). Dynamic mechanical behavior of polymer modified bitumen. *Materials Research Innovations*, **6**, No. 2, 39–43, https://doi.org/10.1007/s10019-002-0159-5.

Rowe, R. K. (2020). Protecting the environment with geosynthetics – the 53rd Karl Terzaghi lecture. *ASCE Journal of Geotechnical and Geoenvironmental Engineering*, **146**, No. 9, 04020081, https://doi.org/10.1061/(ASCE)GT.1943-5606.0002239.

Rowe, R. K. & Abdelaal, F. B. (2016). Antioxidant depletion in high-density polyethylene (HDPE) geomembrane with hindered amine light stabilizers (HALS) in low-pH heap leach environment. *Canadian Geotechnical Journal*, **53**, No. 10, 1612–1627, https://doi.org/10.1139/cgj-2016-0026.

Rowe, R. K. & Rimal, S. (2008). Depletion of antioxidants from a HDPE geomembrane in a composite liner. *ASCE Journal of Geotechnical and Geoenvironmental Engineering*, **134**, No. 1, 68–78, https://doi.org/10.1061/(ASCE)1090-0241(2008)134:1(68).

Rowe, R., Abdelaal, F. & Brachman, R. (2013). Antioxidant depletion of HDPE geomembrane with sand protection layer. *Geosynthetics International*, **20**, No. 2, 73–89, https://doi.org/10.1680/gein.13.00003.

Sá Da Costa, M., Farcas, F., Santos, L. F., Eusébio, M. I. & Diogo, A. C. (2010). Chemical and thermal characterization of road bitumen ageing. *Advanced Materials Science Forum*, **636–637**, No. Pt 1 and 2, 273–279, https://doi.org/10.4028/www.scientific.net/MSF.636-637.273.

Samea, A. & Abdelaal, F. B. (2019). Chemical durability of bituminous geomembranes in heap leaching applications at 55°C. *Geosynthetics 2019*, IFAI, Roseville, MN, USA.

Samea, A. & Abdelaal, F. B. (2023). Effect of elevated temperatures on the degradation behaviour of elastomeric bituminous geomembranes. *Geotextiles and Geomembranes*, **51**, No. 1, 219–232, https://doi.org/10.1016/j.geotexmem.2022.10.010.

Sangam, H. P. & Rowe, R. K. (2002). Effects of exposure conditions on the depletion of antioxidants from high-density polyethylene (HDPE) geomembranes. *Canadian Geotechnical Journal*, **39**, No. 6, 1221–1230, https://doi.org/10.1139/t02-074.

Scheirs, J. (2009). *A Guide to Polymeric Geomembranes: a Practical Approach*. John Wiley and Sons Ltd., West Sussex, UK, 596p.

Sinho, K. P. & Smith, M. E. (2015). Cold climate heap leaching. *Proceedings of the 3rd International Conference on Heap Leach Solutions*, InfoMine, Reno, NV, USA, pp. 409–423.

Steemson, M. & Smith, M. (2009). The development of nickel laterite heap leach projects. In *Proceedings of ALTA 2009 Nickel/Cobalt Conference*. ALTA Metallurgical Services, Perth, Australia, pp. 25–30.

Tauste, R., Moreno-Navarro, F., Sol-Sánchez, M. & Rubio-Gámez, M. (2018). Understanding the bitumen ageing phenomenon: a review. *Construction and Building Materials*, **192**, 593–609, https://doi.org/10.1016/j.conbuildmat.2018.10.169.

Thiel, R. S. & Smith, M. E. (2004). State of the practice review of heap leach pad design issues. *Geotextiles and Geomembranes*, **22**, No. 6, 555–568, https://doi.org/10.1016/j.geotexmem.2004.05.002.

Tian, K., Benson, C. H., Tinjum, J. M. & Edil, T. B. (2017). Antioxidant depletion and service life prediction for HDPE geomembranes exposed to low-level radioactive waste leachate. *ASCE Journal of Geotechnical and Geoenvironmental Engineering*, **143**, No. 6, 1–11, https://doi.org/10.1061/(ASCE)GT.1943-5606.0001643.

Touze-Foltz, N. & Farcas, F. (2017). Long-term performance and binder chemical structure evolution of elastomeric bituminous geomembranes. *Geotextiles and Geomembranes*, **45**, No. 2, 121–130, https://doi.org/10.1016/j.geotexmem.2017.01.003.

Wang, D., Liu, Q., Yang, Q., Tovar, C., Tan, Y. & Oeser, M. (2019a). Thermal oxidative and ultraviolet ageing behaviour of nano-montmorillonite modified bitumen. *Road Materials and Pavement Design*, **22**, No. 1, 121–139, https://doi.org/10.1080/14680629.2019.1619619.

Wang, J., Wang, T., Hou, X. & Xiao, F. (2019b). Modelling of rheological and chemical properties of asphalt binder considering SARA fraction. *Fuel*, **238**, 320–330, https://doi.org/10.1016/j.fuel.2018.10.126.

Wei, H., Bai, X., Qian, G., Wang, F., Li, Z., Jin, J. & Zhang, Y. (2019). Aging mechanism and properties of SBS modified bitumen under complex environmental conditions. *Materials*, **12**, No. 7, 1189, https://doi.org/10.3390/ma12071189.

Wu, S. P., Pang, L., Mo, L. T., Chen, Y. C. & Zhu, G. J. (2009). Influence of aging on the evolution of structure, morphology and rheology of base and SBS modified bitumen. *Construction and Building Materials*, **23**, No. 2, 1005–1010, https://doi.org/10.1016/j.conbuildmat.2008.05.004.

Yang, H., Pang, L., Zou, Y., Liu, Q. & Xie, J. (2020). The effect of water solution erosion on rheological, cohesion and adhesion properties of asphalt. *Construction and Building Materials*, **246**, 118465, https://doi.org/10.1016/j.conbuildmat.2020.118465.

Zhang, F., Yu, J. & Han, J. (2011). Effects of thermal oxidative ageing on dynamic viscosity, TG/DTG, DTA and FTIR of SBS-and SBS/sulfur-modified asphalts. *Construction and Building Materials*, **25**, No. 1, 129–137, https://doi.org/10.1016/j.conbuildmat.2010.06.048.

Zhang, Y., Wei, H. & Dai, Y. (2020). Influence of different aging environments on rheological behavior and structural properties of rubber asphalt. *Materials*, **13**, No. 15, 3376, https://doi.org/10.3390/ma13153376.

Zou, Y., Amirkhanian, S., Xu, S., Li, Y., Wang, Y. & Zhang, J. (2021). Effect of different aqueous solutions on physicochemical properties of asphalt binder. *Construction and Building Materials*, **286**, 122810, https://doi.org/10.1016/j.conbuildmat.2021.122810.

The Editor welcomes discussion on all papers published in Geosynthetics International. Please email your contribution to discussion@geosynthetics-international.com by 15 April 2025